Supplementary information

Shape-controlled gold nanoparticles supported on MoS_2 nanosheets: synergistic effect of thionine and MoS_2 and its application for electrochemical label-free immunosensing

Shao Su,[a] Min Zou,[a] He Zhao,[a] Chengfeng Yuan,[a] Yanan Xu,[a] Chi Zhang,[a] Lihua Wang,[b] Chunhai Fan[b] and Lianhui Wang*[a]

[a]Key Laboratory for Organic Electronics & Information Displays (KLOEID), Institute of Advanced Materials (IAM), National Syngerstic Innovation Center for Advanced Materials (SICAM), Nanjing University of Posts & Telecommunications, 9 Wenyuan Road, Nanjing 210023, China

[b]Division of Physical Biology, Shanghai Institute of Applied Physics, Chinese Academy of Sciences, Shanghai 201800, China.

Preparation of MoS_2

MoS_2 nanosheets were prepared using the intercalation exfoliation method developed by Joensen with some modifications.[1] Under Ar atmosphere, 0.3 g MoS_2 was intercalated with 10 mL n-butyllithium solution at room temperature for about two days. The unreacted n-butyllithium solution and the residual solvent were removed by Ar gas flow. Oxygen-free water was added to exfoliate the Li intercalated MoS_2, and then the suspension was sonicated 1 hour to assist the exfoliation process. Finally, the aqueous dispersion of MoS_2 nanosheets was centrifuged at least twice to remove the LiOH and other soluble impurities.

FTIR spectra of MoS_2, Thi and AuNPs-Thi-MoS_2

The FTIR spectra of MoS_2, Thi and AuNPs-Thi-MoS_2 samples in the range of 4000–400 cm^{-1} are shown in Figure S5. In the FTIR spectra of Thi, the bands around 3440 cm^{-1} and 1640 cm^{-1} are attributed to the stretching vibration and deformation vibration of -NH_2, 2990 cm^{-1} are attributed to the C-H stretching vibration of Thi and the bands around 1427 cm^{-1} were consistent with benzene rings C=C stretching vibration of Thi.[2] In the FTIR spectra of MoS_2, the weak peaks at about 590 cm^{-1} is assigned to Mo-S vibration[3] and the strong peaks at about 1120 cm^{-1} is due to the stretching vibration of S=O. In the FTIR spectra of clovers-shaped AuNPs-Thi-MoS_2, the bands around 1427 cm^{-1} are attributed to the benzene rings C=C stretching vibration of Thi, the bands around 3440 cm^{-1} and 1640 cm^{-1} were consistent with the stretching vibration and deformation vibration of -NH_2 on Thi, which prove the existence of Thi. All these observations demonstrate that Thi is successfully decorated to the AuNPs-Thi-MoS_2 nanocomposites.

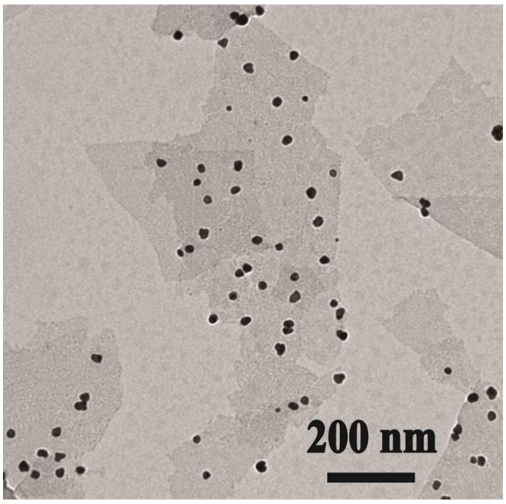

Fig. S1 TEM image of AuNPs-MoS_2 prepared in the absence of Thi.

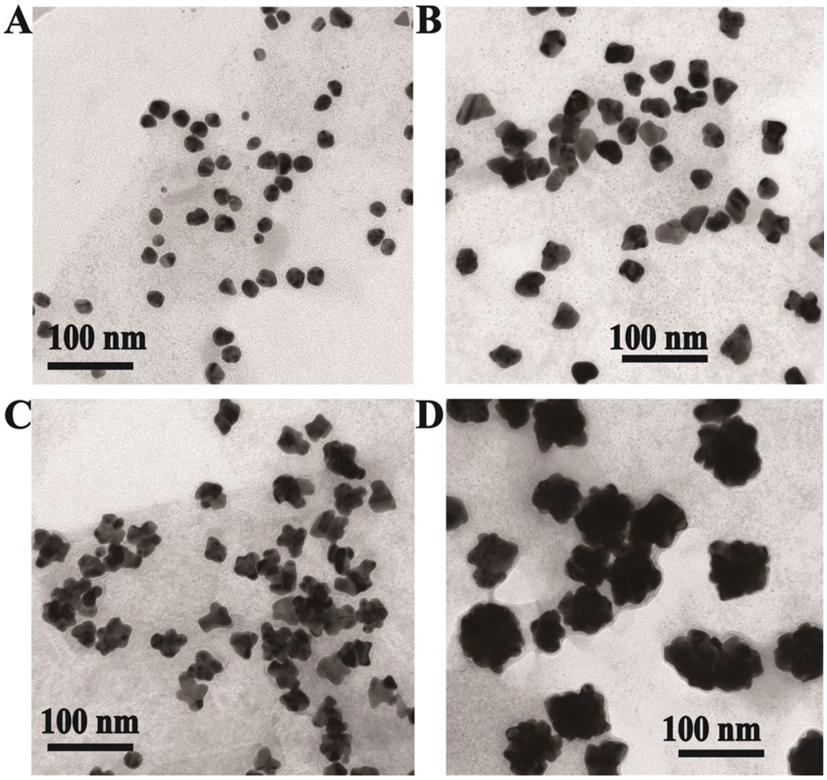

Fig. S2 Enlarged TEM images of AuNPs-Thi-MoS_2 nanocomposites with the addition of varying ratio of MoS_2/Thi (A) 32:1, (B) 32:2, (C) 32:4 and (D) 32:10 with 0.2 mM $HAuCl_4$.

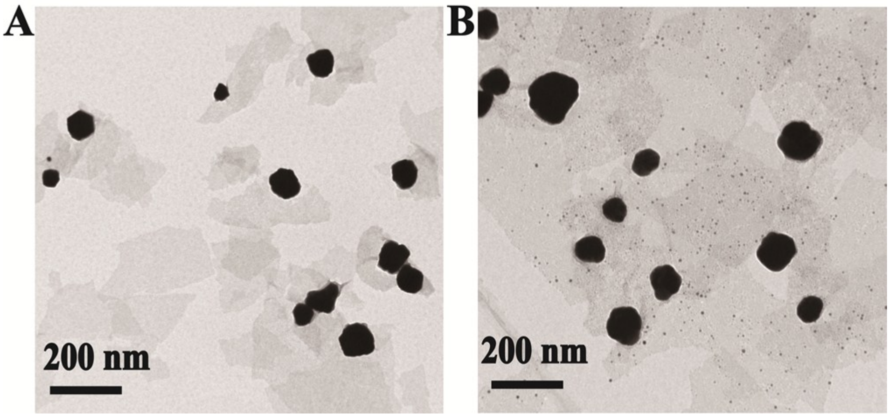

Fig. 3 TEM images of AuNPs-Thi-MoS_2 nanocomposites prepared under different ratio of MoS_2/Thi (A) 32:50 and (B) 32:100 with 0.2 mM $HAuCl_4$.

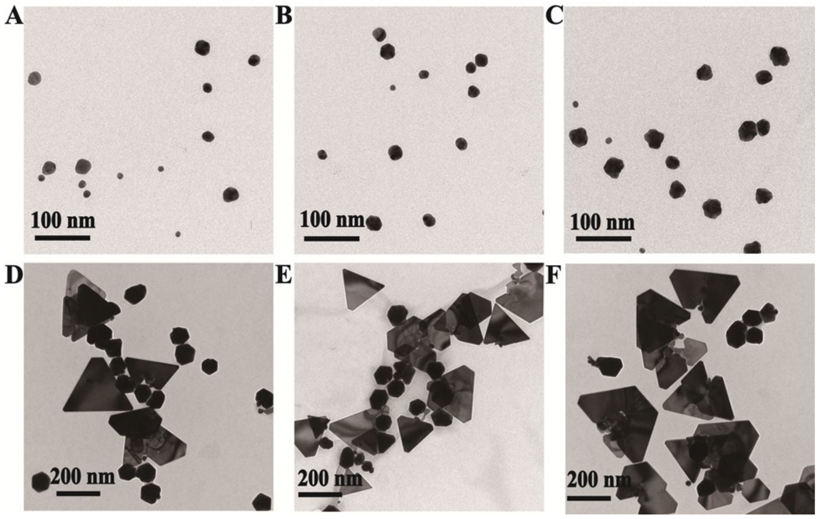

Fig. S4 TEM images of AuNPs prepared by adding different concentration of Thi (A) 1.8 μM, (B) 3.6 μM, (C) 7.2 μM, (D) 18 μM, (E) 90 μM and (F) 180 μM and 0.2 mM $HAuCl_4$ in the absence of MoS_2.

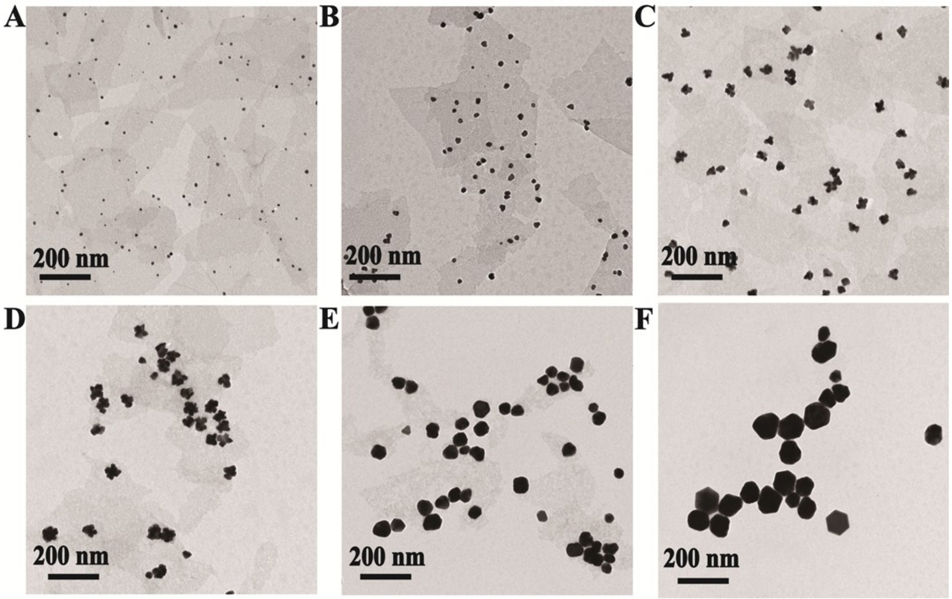

Fig. S5 TEM images of AuNPs-Thi-MoS_2 nanocomposites prepared by changing the concentration of $HAuCl_4$ (A) 0.05 mM, (B) 0.1 mM, (C) 0.15 mM, (D) 0.2 mM, (E) 0.4 mM and (F) 1 mM when the ratio of MoS_2/Thi was 32:4.

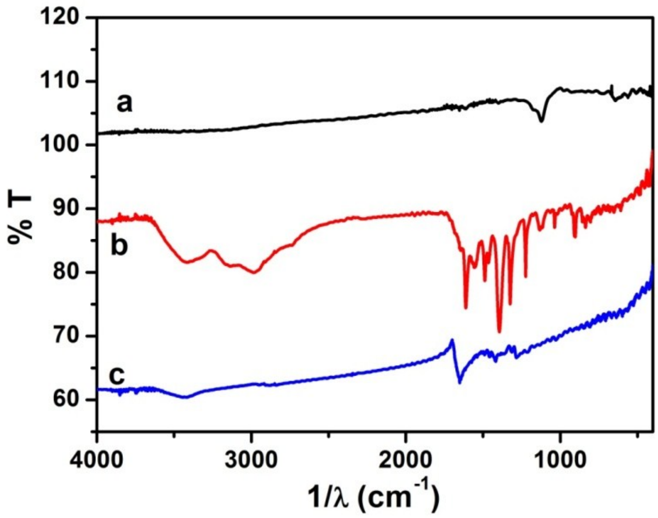

Fig. S6 FTIR spectrum of (a) MoS_2, (b) pure Thi and (c) clovers-shaped AuNPs-Thi-MoS_2 nanocomposites.

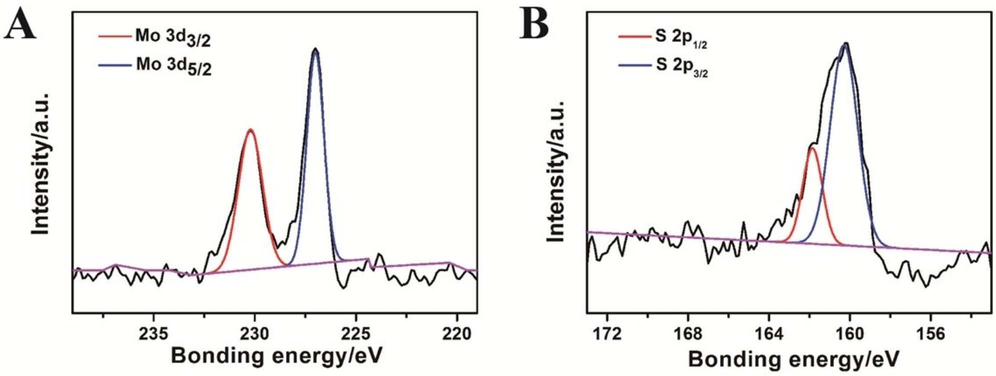

Fig. S7 (A) Mo 3d XPS spectra (B) S 2p XPS spectra of clovers-shaped AuNPs-Thi-MoS_2 nanocomposites.

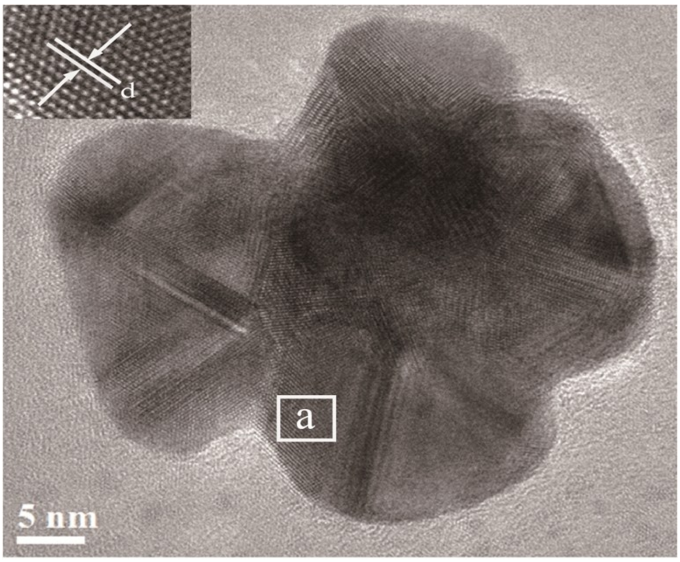

Fig. S8 HRTEM image of clovers-shaped AuNPs-Thi-MoS_2 nanocomposites.

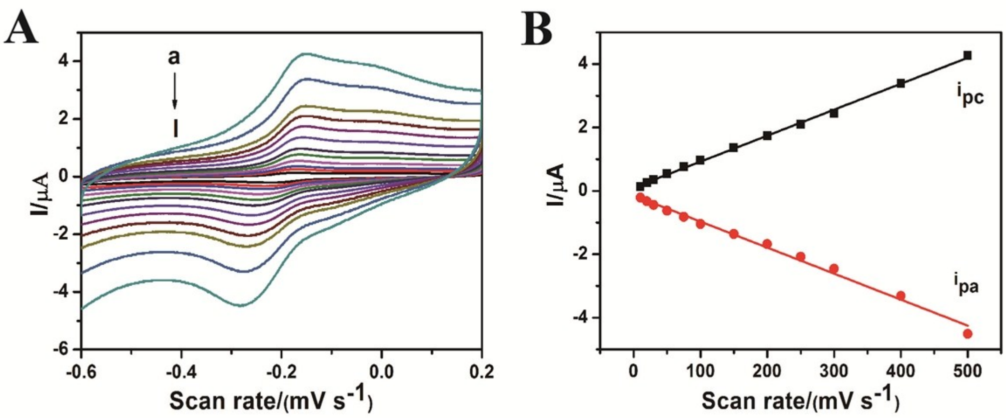

Fig. S9 (A) Cyclic voltammograms of the electrochemical immunosensor at different scan rates (from a to l: 10, 20, 30, 50, 75, 100, 150, 200, 250, 300, 400 and 500 mV s^{-1}). (B) Plots of corresponding anodic and cathodic peak current against scan rate.

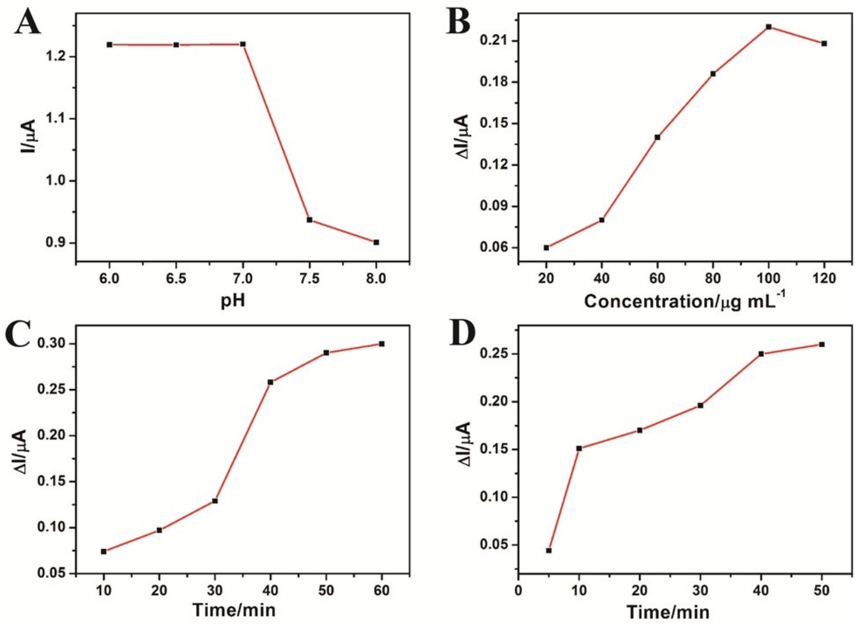

Fig. S10 Effects of (A) pH of detection solution, (B) the concentration of anti-CEA, (C) incubation time of anti-CEA and (D) incubation time of BSA on the immunosensor.

Table S1 The Comparison of analytical performances of the clovers-like AuNPs-decorated Thi-MoS_2 immunosennsor and other reported immunosensors for CEA detection.

The material of sensors	Linear range (ng mL^{-1})	Detection limit (ng mL^{-1})	References
AuNPs/Chits/ CNTs	0.1-200	0.040	4
TiO_2-Gr/Thi/AuNPs	0.01-120	0.010	5
Thi-GS/Ag@Fe_3O_4	0.050 - 16	0.015	6
GNP–Thi–GR	0.01-0.5	0.0040	7
SiO_2/Thi	1-100	0.34	8
rGO-TEPA	0.03-20	0.010	9
AuNP/Fe_3O_4-Chi/PB	0.1-220	0.010	10
AuNPs/MWNT-Chi	0.3-20	0.010	11
Den/AuNP/Thi	10-50	4.4	12
MGO/GHS-Thi	0.01-80	1.0	13
pChit/Thi/GNPs	0.02-160	0.080	14
AuNPs-Thi-MoS_2	0.001-10	0.00052	This work

Abbreviation: [AuNPs] gold nanoparticles; [Chits] chitosans; [CNTs] carbon nanotubes; [TiO_2-

Gr] TiO_2-grapheme; [Thi] thionine; [GS] graphene sheet; [GNPs-Thi-GR] gold nanoparticles-thionine-reduced graphene oxide; [rGO-TEPA] reduced graphene oxide-tetraethylene pentamine; [PB] prussian blue; [Fe_3O_4-Chi] Fe_3O_4 nanoparticles-doped chitosan; [MWCNTs] multi-walled carbon nanotubes; [Den/AuNP] gold nanoparticle-encapsulated Dendrimer; [MGO] magnetic graphene nanosheets; [GHS] nanogold hollow microspheres; [pChit] porous chitosan.

References

1. P. Joensen, R. Frindt and S. R. Morrison, *Mater. Res. Bull.*, 1986, **21**, 457-461.
2. Y. He, Mater. Chem. Phys., 2005, **92**, 134-137.
3. S. Liu, X. Zhang, H. Shao, J. Xu, F. Chen and Y. Feng, *Mater. Lett.*, 2012, **73**, 223-225.
4. X. Zong, G. Wu, H. Yan, G. Ma, J. Shi, F. Wen, L. Wang and C. Li, *J. Phys. Chem. C*, 2010, **114**, 1963-1968
5. K.-J. Huang, Z.-W. Wu, Y.-Y. Wu and Y.-M. Liu, *Can. J. Chem.*, 2012, **90**, 608-615.
6. S. Yu, Q. Wei, B. Du, D. Wu, H. Li, L. Yan, H. Ma and Y. Zhang, *Biosens. Bioelectron.*, 2013, **48**, 224-229.
7. F.-Y. Kong, M.-T. Xu, J.-J. Xu and H.-Y. Chen, *Talanta*, 2011, **85**, 2620-2625.
8. Y. Zhuo, R. Yu, R. Yuan, Y. Chai and C. Hong, *J. Electroanal. Chem.*, 2009, **628**, 90-96.
9. D. Wu, A. Guo, Z. Guo, L. Xie, Q. Wei and B. Du, *Biosens. Bioelectron.,* 2014, **54**, 634-639.
10. H. Chen, J. Tang, B. Su, G. Chen, J. Huang and D. Tang, *Anal. chim. acta*, 2010, **678**, 169-175.
11. K.-J. Huang, D.-J. Niu, W.-Z. Xie and W. Wang, *Anal. chim. acta*, 2010, **659**, 102-108.
12. B. Jeong, R. Akter, O. H. Han, C. K. Rhee and M. A. Rahman, *Anal. chem.*, 2013, **85**, 1784-1791.
13. J. Tang, D. Tang, R. Niessner, G. Chen and D. Knopp, *Anal. chem.*, 2011, **83**, 5407-5414.
14. Y. Liu, R. Yuan, Y. Chai, C. Hong, K. Liu and S. Guan, *Microchim. Acta*, 2009, **167**, 217-224.